Austin Journal of Cancer and Clinical Research

Open Access
Full Text Article

Research Article

Semi-Automated Co-Segmentation of Tumor Volume Using Multimodality PET-CT in Non-Small Cell Lung Cancer (NSCLC)

Li H[1], Bai J[2], Wu X[2], Bhatia SK[1], Abu-Hejleh T[3], Sun W[1], TenNapel MJ[1], Menda Y[4], Mart CJ[1], McGuire SM[1], Flynn RF[1], Buatti JM[1] and Kim Y[1]*

[1]Department of Radiation Oncology, University of Iowa, USA
[2]Department of Electrical and Computer Engineering, University of Iowa, USA
[3]Department of Internal Medicine, University of Iowa, USA
[4]Department of Radiology, Division of Nuclear Medicine, University of Iowa, USA

***Corresponding author:** Yusung Kim, Assistant Professor, Department of Radiation Oncology, Carver College of Medicine, University of Iowa, 200 Hawkins Drive, 01607PFP-W, Iowa City, IA52242, USA, Tel: 001-319-384-9406; Fax: 001-319-356-1530; Email: yusung-kim@uiowa.edu

Received: April 10, 2014; Accepted: May 24, 2014; Published: May 28, 2014

Abstract

Introduction: Lung cancer is the most commonly occurring cancer for both men and women with the highest associated mortality rate. Positron emission tomography and computed tomography (PET-CT) are accurate evaluation modalities in determining lung cancer extent and aggression. An efficient and reliable computerized tumor volume (TV) delineation system, based on PET-CT imaging is needed for accurate tumor response analysis during daily clinical practice and in large clinical trial.

Purpose: To present and validate a novel computer-aided, semi-automatic co-segmentation method for lung tumor volume (co-segmented TV_{PET-CT}) that integrates tumor boundaries on both PET and CT.

Methods and Materials: Eighteen patients were included all of whom had stage III/IV NSCLC had received chemoradiotherapy, PET-CT simulation pre-radiotherapy and a CT scan at 2-4 months follow-up post-radiotherapy. Pre-radiotherapy GTV (pre-GTV) on PET-CT images were retrospectively contoured by two physicians who reached consensus on the volume and then used this as the reference tumor volume. The statistical correlation were analyzed between the reference tumor volume and different segmented tumor volumes; co-segmented TV_{PET-CT}, segmented Tumor Volume on CT alone (TV_{CT}), segmented Tumor Volume on PET alone (TV_{PET}), Tumor Volume ($TV_{SUV2.5}$) delineated using the SUV2.5 threshold, and Tumor Volume ($TV_{SUVmean}$) using the SUV_{MEAN} threshold.

Results: The co-segmented TV_{PET-CT} showed the most significant correlation with pre-GTV (correlation coefficient = 0.993), along with the most favorable ASSD (1.48 ± 0.8 mm) and DSC values (0.85 ± 0.07). $TV_{SUV2.5}$, TV_{CT}, TV_{PET}, and post-GTV significantly correlated with pre-GTV ($P < 0.001$) except for $TV_{SUVmean}$ ($P = 0.42$). Smoking status and histology presented significant correlation with %ΔTV ($P = 0.0273$ and $P = 0.0297$ respectively) while no significant correlations in gender, age, and stage were evident. None of other computer-aided segmented tumor volumes or SUVs correlated with %ΔTV. The overall averaged tumor response rate after chemoradiotherapy in 2 - 4 months is 70 ± 18.6%.

Conclusion: The co-segmented tumor volume on PET-CT was most strongly correlated with two-physician-consensus manual contouring that clinically incorporates PET and CT information.

Keywords: PET-CT; Computer-aided segmentation co-segmentation; Non-small cell lung cancer; PET

Introduction

Lung cancer is the leading cause of cancer-related death in the world [1]. During 2013 it caused 159,260 deaths in the United States [2] with only a 16.3% 5-year overall survival [3]. Eighty-five percent of lung cancers are diagnosed as NSCLC, and 70% of patients present with advanced disease (stage III - IV) [4,5]. Clinical decision making is generally predicted upon tumor response with complete response defined as tumor disappearance, partial response as more than 25% decrease in size measured by CT, stable disease as less than 25% decrease or increase, progressive disease as greater than 25% increase in the tumor diameter using RECIST criteria (response evaluation criteria in solid tumors) [6,7]. Consequently, there is a compelling need for the more accurate measurement of the tumor volume for identifying tumor extent for treatment and quantifying tumor response to treatment.

Studies suggest that the combination of functional (PET) and anatomical imaging (CT) (PET-CT) is a reliable indicator of tumor extent and distribution [1,8]. The use of PET-CT imaging altered the tumor volume delineation of NSCLC in more than 50% of patients when compared with CT-based tumor volume alone [9,10].

Citation: Li H, Bai J, Wu X, Bhatia SK, Abu-Hejleh T, Sun W, et al. Semi-Automated Co-Segmentation of Tumor Volume Using Multimodality PET-CT in Non-Small Cell Lung Cancer (NSCLC). Austin J Cancer Clin Res 2014;1(3): 1013.

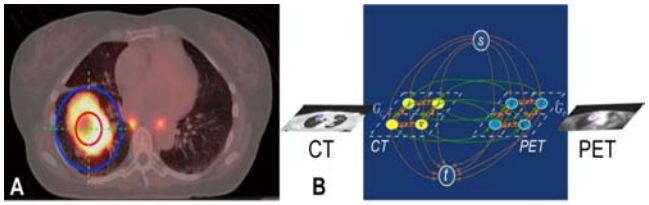

Figure 1: (A) Example slices of the initialization step in the fused image of PET (thermal) and CT (gray scale). The orange sphere completely lies inside the tumor and the blue sphere completely contains the tumor. (B) Graph construction of G with two sub-graphs GC (Graph from CT) and GP (Graph from PET) for the co-segmentation of PET-CT images. Three types of arcs are introduced. The orange arcs encode the boundary terms; the brown arcs encode data terms; and the green arcs enforce the PET-CT context term in the co-segmentation energy function.

Table 1: Patients' characteristics

Gender	Number	Chemotherapy	Number
Male	9	Carboplatin	3
Female	9	Carboplatin + taxol	13
		Carboplatin + etoposide	2
Age	**Number**	**Histology**	**Number**
Mean	58.3 years	Squamous cell	8
Range	(47 – 71 years)	Adenocarcinoma	9
		NSCLC (non-classified)	1
Stage	**Number**	**Prescription dose**	
III	11	Mean	65 Gy
IV	7	Range	(50 - 70 Gy)

Information obtained from combined PET-CT imaging that cannot be obtained from PET only data for lung cancer patients enables the physician to differentiate between anatomic pathological and physiological changes. In radiation oncology practice, manual contouring is still needed in order to delineate the tumor on PET-CT in order to reconcile the two tumor volumes (TVs) defined separately on CT and PET; a process that is time consuming, cumbersome, and error-prone. It also suffers from substantial inter- and intra-observer variability, which limits its utility in large-scale clinical trial research [11]. Reliable auto-segmentation methods that quantitatively analyze PET-CT datasets quickly, robustly, and objectively are presently not clinically available. Existing PET-CT segmentation methods currently in use either work only for a single modality (PET or CT) or work on one image set represented by the fused PET-CT datasets [12].

In this study we propose a novel co-segmentation framework using PET-CT, where TV is co-segmented simultaneously, yet separately, using both PET and CT datasets while admitting the uncertainties described above.

Methods and Materials

PET-CT Co-segmentation algorithm

The process for co-segmenting a tumor volume on PET-CT (co-segmented $TV_{PET\text{-}CT}$) starts from a physician-identified tumor location (Figure 1A). This is accomplished by asking the physician to identify the center of the tumor using three planes on the PET-CT. This is the only step requiring a clinician's input. Afterwards, segmentation is simultaneously performed on each CT and PET image, and globally optimized using the mutual information from both segmentations to generate a co-segmented $TV_{PET\text{-}CT}$ based on the algorithm described by Song *et al.* [13]. To co-segment the tumor from both PET and CT scans, we added a PET-CT context term E_{PET-CT} to the energy functions of CT and PET (Equations (2) and (3) in Ref [13]), which penalizes the segmentation difference between the two image datasets (Figure 1 B). Without loss of generality, we assume that the PET and CT images, I_P and I_C, are registered. Let (p, p') denote a pair of corresponding voxels in I_P and I_C. We penalize the label difference wi th $\delta_{pp'}(f_p^P, f_{p'}^C)$ for p and p'. The PET-CT context term then takes the form:

$$E_{PET-CT}\left(f^P, f^C\right) = \sum_{(p,p')with p\in I_P, p'\in I_C} \delta_{pp'}\left(f_p^P, f_{p'}^C\right)$$

Note that the PET-CT context constraint is soft with $\delta_{pp'}(f_p^P, f_{p'}^C) < +\infty$, which accounts for the tumor boundary differences between PET and CT. The corresponding voxels in PET and in CT could be assigned different labels ("object" or "background") if prominent features present very differently in PET from in CT, which could be caused by imaging uncertainties, registration errors, or both. Our method is thus able to accommodate those uncertainties, further improving its applicability. The energy function of our co-segmentation algorithm is defined as follows:

$$E_{cs}\left(f^P, f^C\right) = E_{PET}\left(f^P\right) + E_{CT}\left(f^C\right) + E_{PET-CT}(f^P, f^C) \qquad (1)$$

We used a more flexible PET-CT context term E_{PET-CT} to make use of the dual modality information [13]. We also minimized the co-segmentation energy function E_{cs} by solving a minimum cost *s-t* cut problem in a transformed graph *G*, which allows a globally optimal solution in low-order polynomial time. To enforce the PET-CT context term E_{PET-CT}, additional inter-sub-graph arcs are introduced between G_P and G_C. Figure 1 B illustrates the construction of the graph *G*, with green arcs encoding the PET-CT context term E_{PET-CT}. The minimum-cost s-t cut in G defines an optimal delineation of tumor volume in both PET and CT images with respect to the energy function (1).

Validation of Co-Segmentation on PET-CT

Records of 649 lung cancer patients were reviewed. A total of 18 patients fulfilled the criteria and their characteristics are listed in Table 1. All patients in this study were enrolled in a NIH approved U01 imaging study. Patients with stage III/IV NSCLC received chemotherapy and lung radiation. The most commonly used chemotherapy regimen was carboplatin and taxol. Other regimens such as carboplatin alone or carboplatin and etoposide were used in a lesser frequency at the physician's discretion. Radiation techniques include intensity-modulated radiation therapy and conventional 3D conformal RT. All patients had PET-CT imaging for simulation and PET-CT (2 patients) or CT (16 patients) at 2-4 months follow-up post-radiation were included. Manual contouring of the pre-GTV was conducted on the registered PET-CT dataset in order to clinically incorporate metabolic PET and morphologic CT information. The tumor contours of the pre-treatment GTV (pre-GTV) and post-treatment residual GTV (post-GTV) were retrospectively generated after thorough consultation between two radiation oncologists. The

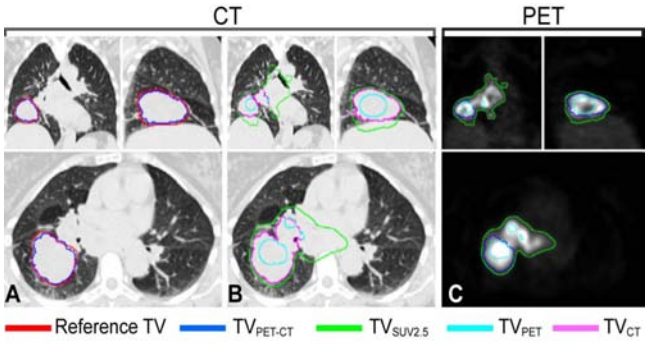

Figure 2: Illustration to show that co-segmented TVPET-CT (blue contour) presents the most favorable match with the reference TV (red) (A) when comparing to other segmented TVs (B); TVPET (Cyan), TVCT (Purple), and TVSUV2.5 (Green). TVPET-CT, TVPET, and TVSUV2.5 are compared on PET imaging (C). **Abbreviations:** co-segmented TVPET-CT = Co-segmented tumor volume on PET-CT, TVSUV2.5 = SUV2.5 threshold based tumor volume, TVCT = Segmented tumor volume on CT alone, and TVPET = Segmented tumor volume on PET alone.

Table 2: Tumor volume, tumor response and SUV characteristics.

Tumor response: GTV		**Pre-GTV: Volume**	
Mean	70%	Mean	160.3 cc
Range	(18.6% - 95%)	Range	(13.8 – 506.9 cc)
Post-GTV: Volume		**Co-segmented GTV on PET-CT: Volume**	
Mean	47.8 cc	Mean	148.9 cc
Range	(0.7 – 242.3 cc)	Range	(9.3 – 490.8 cc)
Mean SUV		**Max SUV**	
Mean	6.6	Mean	16.7
Range	(1.4 – 10.8)	Range	(2.6 – 28)

pre-GTV was used as a reference tumor volume for validation and comparisons of different (semi-)automated tumor volumes. Tumor response after chemoradiotherapy was determined by measuring volume changes between pre- and post-GTV. The percent tumor response was obtained using:

$$\text{tumor response} = \frac{(pre-GTV - post-GTV)}{pre-GTV} \times 100$$

To validate the computer-aided, semi-automatic co-segmented TV_{PET-CT}, we compared the co-segmented TV_{PET-CT} with the reference tumor volume dataset (pre-GTV) (Figure 2). Another four (semi-) automatic segmented tumor volumes were generated and compared (Figure 2): 1) segmented TV_{CT} that is segmented TV on CT alone, 2) segmented TV_{PET} that is segmented TV on PET alone, 3) $TV_{SUV\text{-}MEAN}$ that is segmented based on mean SUV of pre-GTV and 4) $TV_{SUV2.5}$ tumor volume that has a SUV of at least 2.5 [14]. Tumor volume, tumor response and SUV characteristics are listed in Table 2. The Average Symmetric Surface Distance (ASSD) and the Dice Similarity Coefficient (DSC) between each TV metric and the reference dataset were calculated. The DSC between the reference tumor volume which is pre-GTV and a computer-segmented tumor volume (segmented-TV), i.e., either co-segmented TV_{PET-CT}, TV_{PET}, TV_{CT}, $TV_{SUV2.5}$, or $TV_{SUVmean}$, is defined as

$$DSC = \frac{2\,|\,pre-GTV \cap segmentedTV\,|}{|\,pre-GTV\,| + |\,segmentedTV\,|}$$

DSC measures how well two volumes overlap with each other. The value range of the DSC is [0, 1]. A value of 0 represents no overlap at all while a value of 1 represents a perfect overlap of two volumes. The values of the DSC represent similarity between two TVs, thus larger values represent a better geometrical match. The ASSD between two surfaces A and B is defined as

$$ASSD = \frac{\sum_{a\in A}\min_{b\in B}\min_{b\in B} d(a,b) + \sum_{b\in B}\min_{a\in A}\min_{a\in A} d(a,b)}{N_A + N_B}$$

in which a ∈ A and a ∈ B are points on surface A and B, respectively. A Denotes the reference tumor volume surface and *B* denotes the computed surface. *d(a,b)* Is the distance between points *a* and *b*. N_A and N_B are the number of points on surface A and B, respectively. ASSD measures how well the two surfaces align with each other. A smaller ASSD value means better alignment between two surfaces. A value of 0 means perfect alignment between two surfaces. The statistical correlation between different tumor volumes (pre-GTV, co-segmented TV_{PET-CT}, TV_{PET}, TV_{CT}, $TV_{SUV2.5}$) and percent tumor response was tested using Spearman's correlation coefficient. Univariate analysis using linear regression models was performed to assess correlation between percent tumor response and different metrics including different tumor volumes, and SUVs. Other prognostic factors such as gender, age, tumor stage, histology, and smoking status were also analyzed. A Student T-test was used to evaluate the differences of ASSD and DSC between the co-segmented TV_{PET-CT} and other segmented tumor volumes. Statistical analysis was performed using SAS 9.3 (SAS institute Inc., Cary, NC).

Results

Co-segmented Tumor Volume on PET-CT

Co-segmented TV_{PET-CT} was found to show the best statistical correlation with the reference tumor volume dataset (pre-GTV) (R^2 = 0.993) (Figure 3). Except for $TV_{SUV\text{-}MEAN}$ (P = 0.4244 R^2 = 0.040), all other (semi-) automated tumor volumes (co-segmented TV_{PET-CT}, segmented TV_{CT}, segmented TV_{PET}, $TV_{SUV2.5}$, and post-GTV), presented significant correlations with the pre-GTV (P<0.001) (Figure 3).

The co-segmented TV_{PET-CT} had the smallest ASSD values and standard deviations with pre-GTV. On the other hand, it also had the largest DSC values and smallest standard deviations with pre-GTV. According to the paired student T-test, ASSD and DSC of the co-segmented TV_{PET-} 4). Post-GTV was also observed to have statistical correlation with a pre-GTV (P < 0.0001). Figure 2 illustrates $_{CT}$ were significantly better than other tumor metrics including TV_{SUV} $_{2.5}$, $TV_{SUV\text{-}MEAN}$, segmented TV_{CT}, segmented TV_{PET} (P <0.0001) (Figure the tumor volume differences of $TV_{SUV\ 2.5}$, segmented TV_{CT}, segmented TV_{PET}, and co-segmented TV_{PET-CT} when compared to the reference tumor volume dataset.

The overall average tumor response rate after chemoradiotherapy after 2 - 4 months is 70 +/-18.6%. Squamous cell histology responded better compared to adenocarcinoma. The overall tumor response pattern was modeled as post-GTV = -10.00 + 0.36 × pre-GTV (R^2 =

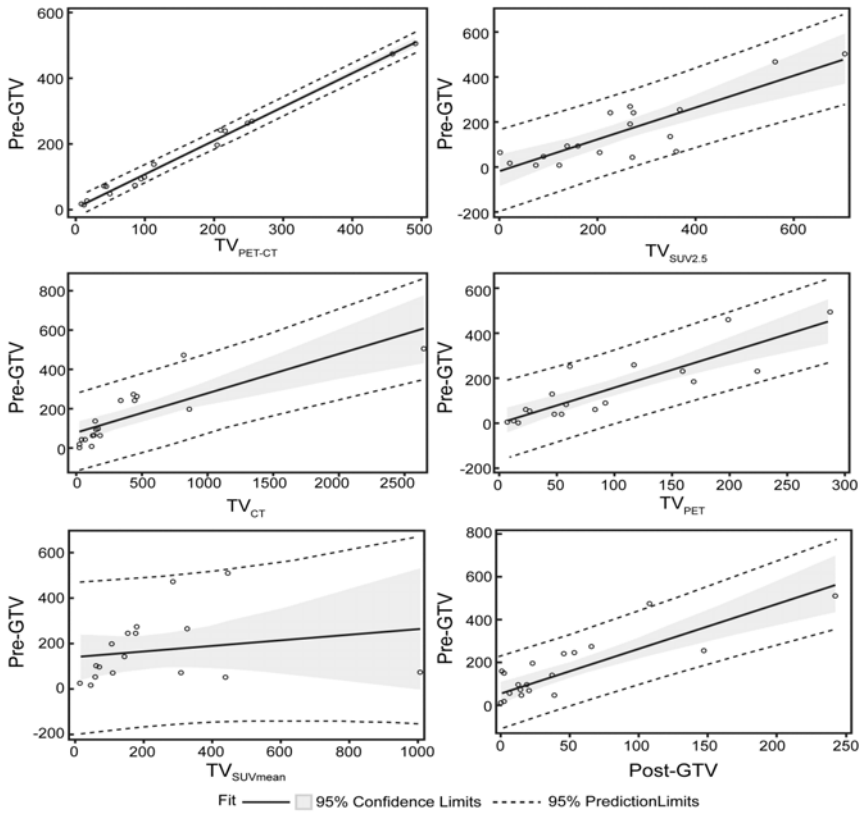

Figure 3: TVSUV2.5, TVCT, TVPET, co-segmented TVPET-CT and post-GTV correlated with physician contoured pre-GTV ($P < 0.001$), while TVSUVmean had no correlation with pre-GTV ($P = 0.42$). **Abbreviations:** TVPET-CT = Co-segmented tumor volume on PET-CT, TVSUV2.5 = SUV2.5 threshold based tumor volume, TVSUVmean = mean SUV of pre-GTV based tumor volume, TVCT = Segmented tumor volume on CT alone, and TVPET = Segmented tumor volume on PET alone.

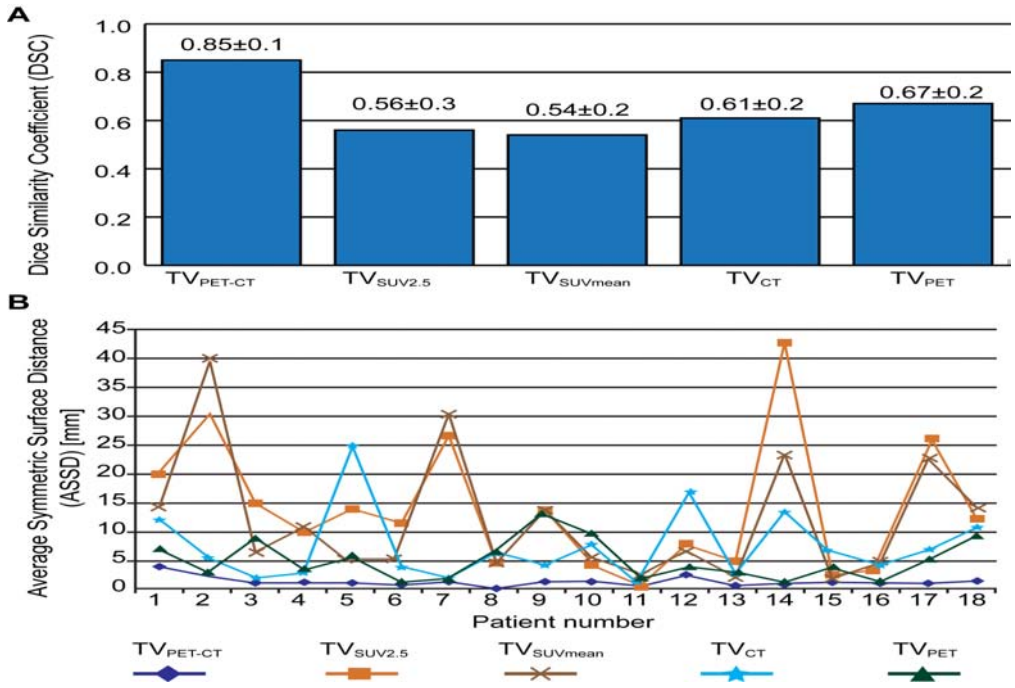

Figure 4: Quantitative performance evaluation on preliminary 18 PET-CT datasets. Average and standard deviation of the DSC values over all datasets (A). The ASSD values for each individual dataset (B).

0.75). Squamous cell and adenocarcinoma tumor response patterns were modeled as post-GTV = 0.71 + 0.20 × pre-GTV (R^2=0.86) and post-GTV = -5.24 + 0.38 × pre-GTV (R^2=0.75) respectively. No significant correlation was found between tumor response and each tumor metric including pre-GTV (R^2=0.047), mean SUV in pre- GTV (R^2=0.124), maximum SUV (R^2=0.008), $TV_{SUV2.5}$ (R^2=0.207), and co-segmented TV_{PET-CT} (R^2=0.204). Univariate analyses were performed to identify any potential predictive factor(s) relating to tumor response. Tumor response was better for squamous cell carcinoma than adenocarcinoma (P=0.0297) and former smokers had more significant tumor response than current smokers (P=0.0273). Gender, age and stage have no impact on tumor response in our study (P=0.9856, P=0.3032, and P=0.5220 respectively).

Discussion

To avoid pathological differences, the analyses in this study were performed on only NSCLC datasets. Tumor response in this study was focused on the primary tumor [15,16] as tumor burden is linked with the survival of NSCLC patients [10,17]. If ^{18}F-FDG PET datasets are available before and after therapy, tumor response can be also evaluated using the criteria of the European Organization for Research and Treatment of Cancer (EORTC) [18]. Antoch [19]. Proposed a tumor response evaluation method utilizing both RECIST criteria [6] and EORTC criteria. For instance, if either the CT or the PET dataset suggests no change but the other imaging modality indicates a partial response, then the final decision is based upon the density of the lesion on CT as measured by Hounsfield Units (HU). They reported tumor response using this combined criteria with an overall accuracy of 95% after 1 month of gefitinib therapy [19]. The accuracy of PET and CT alone were 85% and 44%, respectively [19]. Due to the lack of post-therapy PET datasets, tumor response in this study was quantified as percent tumor volume changes on CT. No significant correlation was found between percent tumor response based on CT and each tumor metric; pre-GTV (P=0.39), mean SUV (P=0.15), $TV_{SUV\,2.5}$ (P=0.25), maximum SUV (P=0.74) and co-segmented TV_{PET-CT} (P=0.88). The predictive power of the proposed co-segmented TV_{PET-CT} datasets over current metrics, e.g. SUV and tumor volume on either CT or PET, remains to be explored when using EORTC and RECIST criteria combined. In addition, its prognostic power over progress free tumor control and overall survival should be evaluated through a prospective clinical trial.

A rigorous and robust TV delineation is essential in order to achieve the high level of predictive certainty for tumor response assessment, especially in patients receiving high-dose RT such as stereotactic body RT. In comparison with manual contouring and computer-aided TV segmentation, the semi-automated, segmented TV was found to be a more accurate technique with less inter observer variation, and remained consistent under varying imaging conditions [20]. The segmentation technique presented the least systematic bias: it showed a mean percent error of 0.05% compared to 25% when using a threshold technique [21].

None of the current prognostic PET-CT assays integrate the morphologic information obtained from CT to define the tumor extent, especially for the primary lung tumor [21]. All assays utilize PET information only. All current prognostic assays are restricted by the uncertainties and limitations imposed by PET only imaging. Manually delineating the tumor volume solely on CT images predicts overall and cause-specific survival, as well as local tumor control in NSCLC patients when using 3D conformal radiotherapy [22]. The current TNM staging system measures only one dimension in relation to the total size of a tumor on CT, instead of measuring the tumor volume in 3-D [7,23]. No prognostic assay has been proposed to integrate the functional with the morphologic information from PET to CT datasets. The full utility of integrating functional and morphologic information from PET-CT images sets as proposed in this prognostic assay using co-segmented tumor volume remains to be explored. In this study, the co-segmented tumor volume was generated using a computer-aided, semi-automatic segmentation method. This approach has the potential to shift the current prognostic assay paradigm in two ways. Firstly, it significantly improves the accuracy of identifying the tumor extent. The segmentation technique presents the least systematic bias; it shows a mean percent error of 0.05% compared to 25% when using a threshold technique [21]. Secondly, a semi-automatic process makes it widely applicable to prognostic staging, diagnosis, and large-scale clinical trials. However, current PET-CT segmentation methods either work only for a single modality or work for the fused PET-CT datasets [12] that require stringent registration between PET and CT, which is impractical. Even with an integrated PET-CT scanner, the acquired PET and CT images may not be well aligned due to the longer acquisition time of the PET scan. Furthermore, due to the different imaging mechanisms, the tumor boundary defined in PET images is not identical to that defined in CT images. The presented co-segmentation method allows the quantitative analysis of PET-CT datasets using tumor extent information from both functional and morphologic imaging.

The results of this study have some limitations that require further research and should be considered carefully prior to further research or clinical application. These limitations are: 1. Accurate segmentation using this method is only valid in lung cancer patients because the CT co-segmentation portion relies significantly on the CT density difference between the tumor and the surrounding tissues on CT images. Theoretically, using this method will be less effective in patients with bulky mediastinal or hilar lymphadenopathy without a distinct primary tumor. Further applications in other anatomical tumor sites will require rigorous testing. 2. This study revealed an average tumor response time of 2-4 months after therapy. These results are based on 70% of the pre-chemoradiation and post-chemoradiation datasets being available for study. However, this statement should be viewed cautiously considering the difficulty of differentiating between residual tumor and treatment-induced lung fibrosis on post-treatment CT images only. Tumor response associated with surgery and/or chemotherapy requires further investigation.

Conclusion

Globally optimized co-segmented tumor volumes on PET-CT presented the most significant correlation (R^2 = 0.993) with the physician's reference contouring. This suggests potential use in clinical practice for draft contouring and invites its validation as an imaging tool in a large scale clinical trial for tumor response assessment. Average local tumor response in 2 - 4 months for advanced stage NSCLC after chemoradiotherapy was 70%.

Acknowledgement

The authors want to express their gratitude to Gareth Smith and Kellie Bodeker for their help editing the figures and identifying subjects. An abstract of this manuscript was partly presented at ASTRO 2013, Atlanta, Georgia.

References

1. Pastorino U, Bellomi M, Landoni C, De Fiori E, Arnaldi P, Picchio M, et al. Early lung-cancer detection with spiral CT and positron emission tomography in heavy smokers: 2-year results. Lancet. 2003; 362: 593-597.
2. Siegel R, Ma J, Zou Z, Jemal A. Cancer statistics, 2014. CA Cancer J Clin. 2014; 64: 9-29.
3. U.S. National Institutes of Health. National Cancer Institute: SEER Cancer Statistics Review 1973-2008. 2008.
4. Traynor AM, Schiller JH. Systemic treatment of advanced non-small cell lung cancer. Drugs Today (Barc). 2004; 40: 697-710.
5. Yang K, Wang YJ, Chen XR, Chen HN. Effectiveness and safety of bevacizumab for unresectable non-small-cell lung cancer: a meta-analysis. Clin Drug Investig. 2010; 30: 229-241.
6. Eisenhauer EA, Therasse P, Bogaerts J, Schwartz LH, Sargent D, Ford R, Dancey J. New response evaluation criteria in solid tumours: revised RECIST guideline (version 1.1). Eur J Cancer. 2009; 45: 228-247.
7. van Rens MT, de la Rivière AB, Elbers HR, van Den Bosch JM. Prognostic assessment of 2,361 patients who underwent pulmonary resection for non-small cell lung cancer, stage I, II, and IIIA. Chest. 2000; 117: 374-379.
8. Caldwell CB, Mah K, Skinner M, Danjoux CE. Can PET provide the 3D extent of tumor motion for individualized internal target volumes? A phantom study of the limitations of CT and the promise of PET. Int J Radiat Oncol Biol Phys. 2003; 55: 1381-1393.
9. Ciernik IF, Dizendorf E, Baumert BG, Reiner B, Burger C, Davis JB, Lütolf UM. Radiation treatment planning with an integrated positron emission and computer tomography (PET/CT): a feasibility study. Int J Radiat Oncol Biol Phys. 2003; 57: 853-863.
10. Bradley J, Thorstad WL, Mutic S, Miller TR, Dehdashti F, Siegel BA, Bosch W. Impact of FDG-PET on radiation therapy volume delineation in non-small-cell lung cancer. Int J Radiat Oncol Biol Phys. 2004; 59: 78-86.
11. Weber WA, Figlin R. Monitoring cancer treatment with PET/CT: does it make a difference? J Nucl Med. 2007; 48 Suppl 1: 36S-44S.
12. Yu H, Caldwell C, Mah K, Mozeg D. Coregistered FDG PET/CT-based textural characterization of head and neck cancer for radiation treatment planning. IEEE Trans Med Imaging. 2009; 28: 374-383.
13. Song Q, Bai J, Han D, Bhatia S, Sun W, Rockey W, Bayouth JE. Optimal co-segmentation of tumor in PET-CT images with context information. IEEE Trans Med Imaging. 2013; 32: 1685-1697.
14. Okada M, Shimono T, Komeya Y, Ando R, Kagawa Y, Katsube T, et al. Adrenal masses: the value of additional fluorodeoxyglucose-positron emission tomography/computed tomography (FDG-PET/CT) in differentiating between benign and malignant lesions. Annals of nuclear medicine. 2009; 23: 349-354.
15. Berghmans T, Dusart M, Paesmans M, Hossein-Foucher C, Buvat I, Castaigne C, et al. Primary tumor standardized uptake value (SUVmax) measured on fluorodeoxyglucose positron emission tomography (FDG-PET) is of prognostic value for survival in non-small cell lung cancer (NSCLC): a systematic review and meta-analysis (MA) by the European Lung Cancer Working Party for the IASLC Lung Cancer Staging Project. J Thorac Oncol. 2008; 3: 6-12.
16. Paesmans M, Berghmans T, Dusart M, Garcia C, Hossein-Foucher C, Lafitte JJ, et al. Primary tumor standardized uptake value measured on fluorodeoxyglucose positron emission tomography is of prognostic value for survival in non-small cell lung cancer: update of a systematic review and meta-analysis by the European Lung Cancer Working Party for the International Association for the Study of Lung Cancer Staging Project. J Thorac Oncol. 2010; 5: 612-619.
17. Brundage MD, Davies D, Mackillop WJ. Prognostic factors in non-small cell lung cancer: a decade of progress. Chest. 2002; 122: 1037-1057.
18. Young H, Baum R, Cremerius U, Herholz K, Hoekstra O, Lammertsma AA, et al. Measurement of clinical and subclinical tumour response using [18F]-fluorodeoxyglucose and positron emission tomography: review and 1999 EORTC recommendations. European Organization for Research and Treatment of Cancer (EORTC) PET Study Group. Eur J Cancer. 1999; 35: 1773-1782.
19. Antoch G, Kanja J, Bauer S, Kuehl H, Renzing-Koehler K, Schuette J, Bockisch A. Comparison of PET, CT, and dual-modality PET/CT imaging for monitoring of imatinib (STI571) therapy in patients with gastrointestinal stromal tumors. J Nucl Med. 2004; 45: 357-365.
20. Werner-Wasik M, Nelson AD, Choi W, Arai Y, Faulhaber PF, Kang P, Almeida FD. What is the best way to contour lung tumors on PET scans? Multiobserver validation of a gradient-based method using a NSCLC digital PET phantom. Int J Radiat Oncol Biol Phys. 2012; 82: 1164-1171.
21. Chao F, Zhang H. PET/CT in the staging of the non-small-cell lung cancer. J Biomed Biotechnol. 2012; 2012: 783739.
22. Bradley JD, Ieumwananonthachai N, Purdy JA, Wasserman TH, Lockett MA, Graham MV, et al. Gross tumor volume, critical prognostic factor in patients treated with three-dimensional conformal radiation therapy for non-small-cell lung carcinoma. Int J Radiat Oncol Biol Phys. 2002; 52: 49-57.
23. Adebonojo SA, Bowser AN, Moritz DM, Corcoran PC. Impact of revised stage classification of lung cancer on survival: a military experience. Chest. 1999; 115: 1507-1513.

Austin J Cancer Clin Res - Volume 1 Issue 3 - 2014
ISSN : 2381-909X | www.austinpublishinggroup.org

Citation: Li H, Bai J, Wu X, Bhatia SK, Abu-Hejleh T, Sun W, et al. Semi-Automated Co-Segmentation of Tumor Volume Using Multimodality PET-CT in Non-Small Cell Lung Cancer (NSCLC). Austin J Cancer Clin Res 2014;1(3): 1013.